Azimuth-Dependent Site Amplification

HUNG-CHIE CHIU[1] AND HUEY-CHU HUANG[2]

ABSTRACT

The strong motion accelerograms recorded at two stations of SMART-1 array have been analyzed to investigate azimuth-dependent site amplification. Fifteen earthquakes which triggered both accelerographs at rock site E02 and soil site E01 were selected for this study. We measure the spectral ratio of E01 to E02 in a window which includes direct S waves. Since ground motions at the rock site are less modified by the site effects and E02 and E01 are only 2 *km* apart, the spectral ratio of the soil site to the rock site will cancel most of source and raypath effects and reflect the site amplification of the soil site.

These earthquakes are divided into 10 groups. The earthquakes in the same group have similar epicentral distance and backazimuth. Our studies show that different groups have different spectral ratios and no systematic changes have been found among the groups. In the same group, all earthquakes were expected to have the similar spectral ratio. However, similar spectral ratios were only found in some groups over some limited frequency ranges. These discrepancies are interpreted as the results of near-source and non-linear effects.

1. INTRODUCTION

Site amplification is a complicate effect. It depends not only on site conditions but also input motions. There are two major factors which can be considered as site conditions. One is the material of the medium and the other one is the geometry of topography and subsurface structures. Seed *et al.* (1976) classified the observed spectral accelerations into four categories based on the type of top-layer medium, namely, (1) soft to medium clay and sand, (2) deep cohesionless soil, (3) stiff soil, and (4) rock. Campbell (1989) used another set of four types of site condition to characterize the site effects and included them into his regression analysis of peak horizontal acceleration. In his classification, the site conditions were grouped as (1) alluvium, (2) soft rock, (3) hard rock, and (4) shallow soil. Although both of these broad classifications are not enough to characterize the site condition, both of

[1] *Institute of Earth Sciences, Academia Sinica*
[2] *Institute of Geophysics, National Central University*

their works have shown that medium of the top layer at site may strongly affect the site amplification.

Effects of the geometry of topography and subsurface structure on site amplification were mostly found in analytic solutions for simple models and in numerical simulation. One well-known observation of topography effect is the over $1g$ recording at Pacoima Dam during the San Fernando earthquake of 1971. The analytic and numerical studies of the topography and subsurface structure effects on the site amplification were rapidly developed in the past two decades. For examples, Boore (1972) calculated the response of normal incident plane SH wave caused by a triangular ridge and showed that the motion at the ridge crest can be amplified up to about 70%. Trifunac (1973), Wong (1975) and Chiu and Huang (1992) studied the canyon effects on the ground motion and demonstrated that there was amplification at the edge and deamplification at the bottom of the canyon. The canyon also produces a shielding effect which may cause strong deamplification at the far side of the canyon. For a detailed discussion of SH, P, SV and Rayleigh waves incident on a variety of two and three dimensional irregular topography and subsurface structures, one can refer an excellent review paper (Aki, 1988). All these works have shown that the geometry of site is also an important effect. Furthermore, Bonamassa and Vidale (1991) have pointed out that site effect may amplify the motion of scattered waves in one preferred direction, thus constituting another effect on site condition.

Input motions play the same role in site amplification as that of site condition. The types of waves, frequency content, incident angle and strain level of the input motions have been recognized as being able to affect site amplification. Many literatures have discussed this problem. For example, Burridge *et al.* (1980) had shown that the peak amplification decreases with increasing incident angle. Kamiyama and Yanagiswa (1986) analyzed frequency-dependent amplification, Trifunac and Lee (1990) studied the frequency dependent attenuation. Burridge *et al.*, (1980); Wong, (1982) demonstrated that the same site would response differently depending on the types of incident waves. All these studies have showed that incident angle, frequency content and type of incident waves are important factors in the site amplification. One more important factor which is less understood so far is the non-linear behavior of the medium. This effect depends on the medium itself and the strain level of the input motion. As the amplitude of the input motion is increased, the shear modulus and damping result in non-linear hysteretic behavior. This effect will shift the input motion to longer period and reduce the peak response. The non-linear effect only occurs in high potential medium with large ground motion, therefore, it is very important in site amplification.

In the present paper, we address a new problem: How the backazimuth will affect the site amplification? This problem involves several factors discussed above. We use SMART-1 data at two nearby stations (E01 and E02) to investigate it. E01 is on an alluvium site while E02 is on a rock site. This data set allows us to cancel source and ray path effects, therefore, provides a great opportunity to look the effect of backazimuth on the site amplification.

2. SEISMIC DATA AND SITE GEOLOGY

The SMART1 array, located in the Lanyang plain, northeastern Taiwan, consists of a center site (C00) and 36 stations on three concentric circles labeled as inner I, middle M, and outer O. This array started its operation in September 1980. In June 1983, two additional stations (E01 and E02) were added to extend the array to the edge of the Lanyang plain (Figure 1). E02 is on a rock site and all other stations are on soil sites. By December 1990, 61 earthquakes were recorded by this array, and fifteen of them which triggered both stations E01 and E02 are selected in this study. Table 1 gives the seismic parameters of

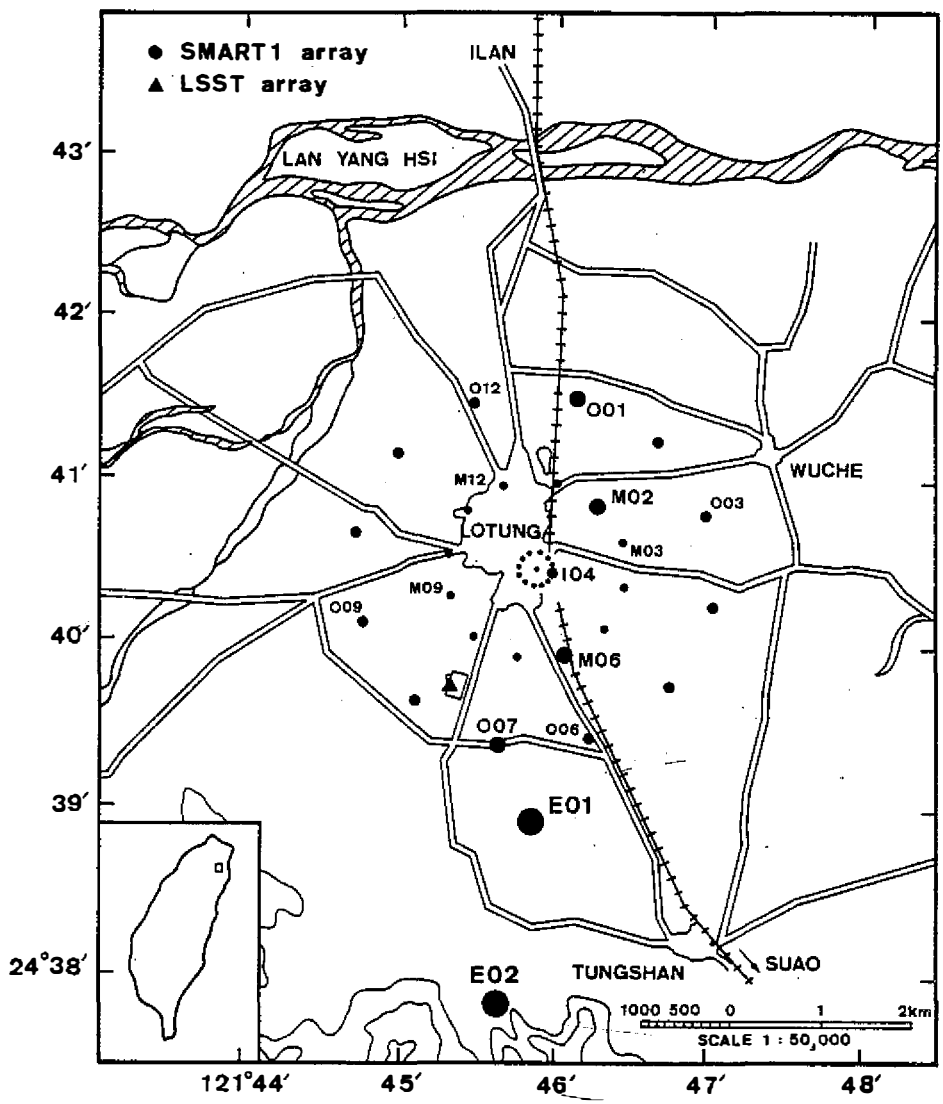

Fig. 1. Layout of the SMART1 array in Northeastern Taiwan. The rock site E02 is on the southern edge of the Lanyang plain and the soil site E01 is between E02 and three concentric circles.

Table 1. Earthquakes used in this study

Group No.	Event No.	Origin Time (GMT)	EpiCenter		Mag. (ML)	Depth (KM)	Δ (KM)	θ (deg.)
			Longitude	Latitude				
1	35	1985 08 12 12:00:33.26	121-47.10E	24-42.71N	5.7	8.0	7.3	16.6
2	39	1986 01 16 13:04:31.97	121-57.67E	24-45.77N	6.5	10.2	23.6	57.6
3	29	1984 04 23 22:35:04.03	122-05.34E	24-47.31N	6.0	8.7	36.3	64.7
4	32	1985 06 12 13:23:13.3	122-13.93E	24-35.41N	5.3	5.3	47.8	97.7
	33	1985 06 12 17:22:50.84	122-11.68E	24-34.38N	6.5	3.3	44.4	100.8
	36	1985 09 20 15:01:24.03	121-11.87E	24-31.97N	6.3	6.1	45.7	106.2
5	44	1986 07 30 11:38:31.7	121-47.73E	24-38.38N	4.9	2.3	3.1	108.7
	43	1986 07 30 11:31:47.53	121-47.65E	24-37.73N	6.2	1.6	3.8	125.2
6	25	1983 09 21 19:20:40.73	121-18.99E	23-56.29N	6.8	18.0	96.6	144.4
7	34	1985 08 05 13:00:38.6	121-52.97E	24-22.95N	5.8	1.3	31.8	157.9
	37	1985 10 26 03:30:39.11	121-49.70E	24-24.67N	5.3	1.7	27.1	165.8
8	45	1986 11 14 21:20:01.2	121-49.99E	23-59.91N	6.8	13.9	76.5	174.5
9	54	1987 11 10 04:33:09.18	121-43.42E	24-25.11N	5.2	34.5	25.9	189.6
10	41	1986 05 20 05:37:31.69	121-37.04E	24-02.90N	6.2	21.8	68.2	192.7
	40	1986 05 20 05:25:49.58	121-35.49E	24-04.90N	6.5	15.8	65.2	195.7

Δ : Distances between station (E01) and epicenters.
θ : Backazimuths of epicenters to E01.

events. Figure 2 shows the locations of the SMART1 array and 15 epicenters as listed in Table 1. These earthquakes cover a range of epicentral distance from 3.1 to 96.6 *km*, and span local magnitudes from 4.9 to 6.9. Each accelerograph consists of a triaxial force-balance accelerometer and a digital recorder with 12-bit resolution at a rate of 100 samples per second. For convenience of discussion, these events are divided into ten groups according to their epicentral distance and backazimuth. Among these groups, groups 4 (events 32, 33 and 36), 5 (events 43 and 44), 7 (events 34 and 37) and 10 (events 40 and 41) consist of more than one event and all others groups only have one event. In the same group, all earthquakes have similar epicentral distance and backazimuth. The backazimuth of these groups are monotonously increased, from group 1 (16.6°) to (195.7°).

The subsurface geology beneath the SMART1 array was divided into three layers. Recent alluvium overlies more consolidated Pleistocene strata and a Miocene basement (Chiang, 1976). In Wen and Yeh's (1984) model, the top layer is further divided into two sublayers. The P-wave velocity of the upper sublayer is 0.43 – 0.76 *km / sec* with a thickness of 0.01 *km* and that of the lower sublayers is 1.4 – 1.7 *km / sec* with a thickness of 0.05 *km*. The Pleistocene strata have velocities ranging from 1.8 – 2.0 *km / sec*. The velocity for the basement is 3.3 *km / sec*. Generally, the thickness of strata increase from west to east and more gently increase from south to north. For the shallow subsurface structure (< 50 *m*), the geological conditions under this array are relatively uniform.

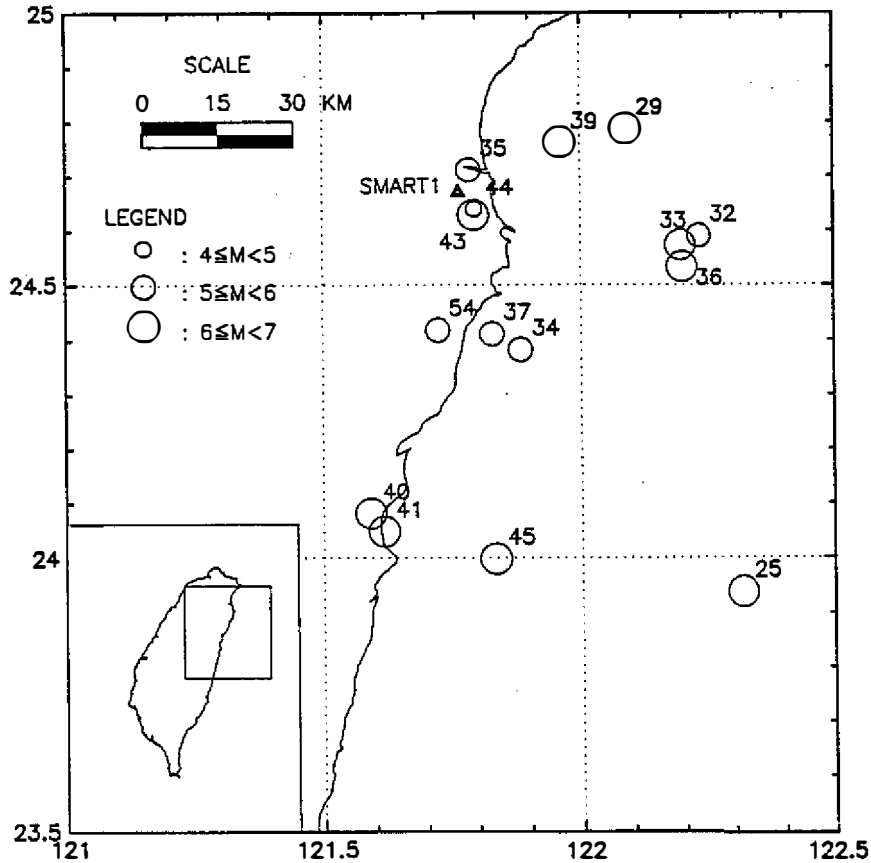

Fig. 2. Epicenter locations of fifteen earthquakes selected in this study.

3. METHOD

We measure the ratio of the total spectra of E01 to that of E02 to examine the azimuth-dependent site amplification. For all events except event 45, we applied a *5-second* windows (Figure 3) with a cosine taper to extract the direct S waves. For event 45, the rupture process of the corresponding fault seems to be more complicate and to last longer, so we used a *10-second* window. Modiano (1980) has shown that the smooth modules of the Fourier spectrum of a seismic signal varies very slowly along the seismogram. We checked it again using the SMART-1 data and obtained similar results. Thus it is not necessary to identify precisely the arrival of the S wave. Although the spectra have been shown to be stable when we shift the window backward and forward over a range, the wide window has extracted more signal than only direct S wave. Those signals following the direct S wave will generate noise in the spectral ratio.

We used the spectral ratio is mainly for removing the source and raypath effects to reveal the site effect. The Fourier spectra are the same as the observed accelerograms which combined the source, raypath and site effects. In general, it is very difficult to separate these

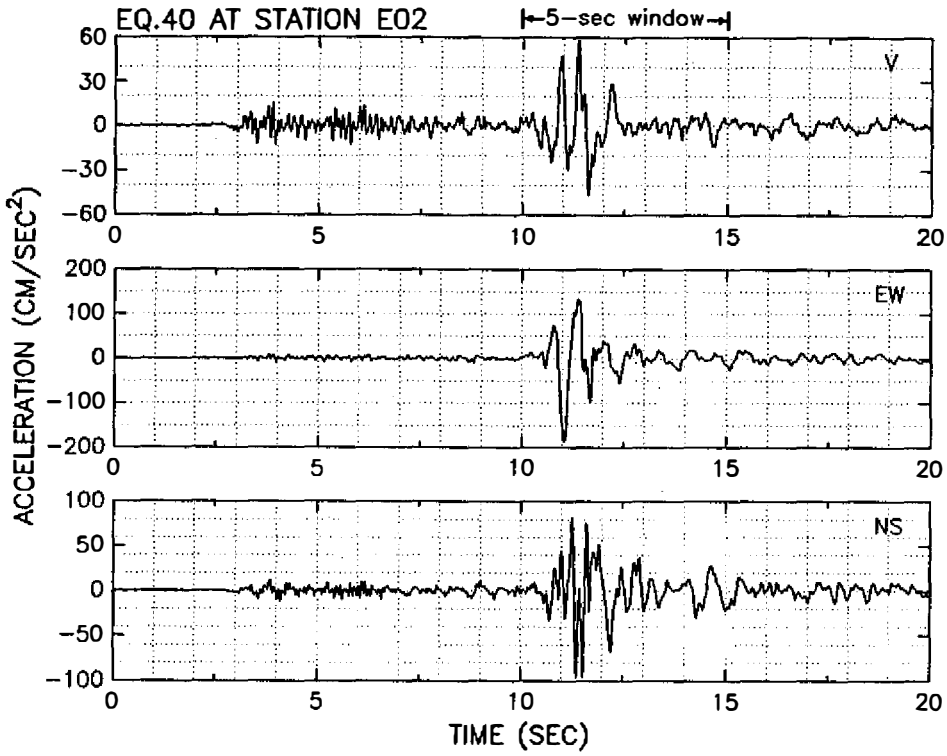

Fig. 3. Three-component waveforms of Earthquake 40 at station E02 and window selected to extract S waves.

effects. However, if any two sites are close enough and their epicentral distance is relatively much larger than the dimension of the corresponding earthquake fault, the spectral ratio of these two sites will cancel the source and raypath effects and approximate the ratio of the site effects only. Furthermore, if we choose the rock site as a reference (denominator in the ratio), this ratio will further reveal the site effects of the other station (nominator in the ratio).

Instead of using the spectral ratio of individual components, we used the total spectral ratio in this study. The main purpose was to try to compare the spectral ratios among these events on the same basis and to avoid error caused by the misalignment of accelerometers. The total spectrum F_{tot} is defined as:

$$F_{tot} = \sqrt{F_V^2 + F_{EW}^2 + F_{NS}^2} \tag{1}$$

where F_V, F_{EW}, and F_{NS} represent the vertical, E-W and N-S components of Fourier spectra respectively. The total spectra are independent of the orientation of the instrument, therefore, we can ignore the effects of instrument misalignment. Furthermore, the total spectra can avoid biased distribution of ground motions on two horizontal components. Since one component of accelerometer is chosen to point to the north not to the epicenter. If we only

used one of the horizontal components, in fact, we would be comparing spectral ratios of different projections.

The spectral ratio r of two stations used in his paper is defined as:

$$r = F_{tot}^1 / F_{tot}^2 \tag{2}$$

where F_{tot}^1 and F_{tot}^2 are the total spectra at stations 1 and 2.

Since the ratio measures the difference of the site effects at two sites, some intrinsic and numerical errors that may affect the estimation of site amplification should be minimized. These factors include the orientation of instruments, background noise, and troughs of the spectra in the denominator. We have eliminated the error caused by the misalignment of instruments by choosing total spectra. In order to estimate the error caused by the background noise, we did a microtremor survey at site *E*01 and *E*02. During several measurements, we only found one unidentified burst detected at *E*01 with peak of 0.63 cm/sec^2. In all other records, the background noises at these two stations are less than 0.05 cm/sec^2. Two typical records at these two stations are shown in Figure 4. The total Fourier spectra of 15 earthquake accelerations and 23 sets of noise measured at E01 and E02 are shown in Figure 5. In general, the noise at E01 is larger than that at E02 but high frequency components were found to be rich at station E02. Since this high frequency part is out of the range of interest (0 – 10 *Hz*) in this paper, the high frequencies are not shown in Figure 5. Most Fourier spectra at E01 fall between 1 to 100 *cm / sec* over the whole frequency range, while the noises are less than 0.01 *cm / sec* in most cases. At E02 the spectra of acceleration also cover a range from 1 to 100 *cm / sec* and the background noise are less than 0.01 *cm / sec*. Based on these results, background noise should not be a major factor that may contaminate the spectral ratio.

The other source of error may come from the small value of spectrum (trough in the spectrum) in the denominator. When the denominator has a small value, a small amount of error in the nominator could be significantly magnified. In order to minimize this error, we let all the denominators which are less than 2 *cm / sec* to 2 *cm / sec*. This modification will cause the true peaks to become smaller, but it can effectively remove most pseudo peaks that appear in the spectral ratio.

The detailed steps for calculating the spectral ratios are summarized as follows:

1. From each seismogram, 5-*second* (or 10-*second*) of the wave train which covers the S waves were extracted with a rectangular window with a 0.5 *sec* cosine taper at each end (Figure 3).
2. Fourier transforms of these extracted wave train at each component were obtained using a FFT routine.
3. The total spectra for each event at every station are calculated using equation (1).
4. A frequency-by-frequency ratio was then constructed for each event. If the value of F_{tot}^2 is less than 2 *cm / sec* then F_{tot}^2 is set equal to 2 *cm / sec*.

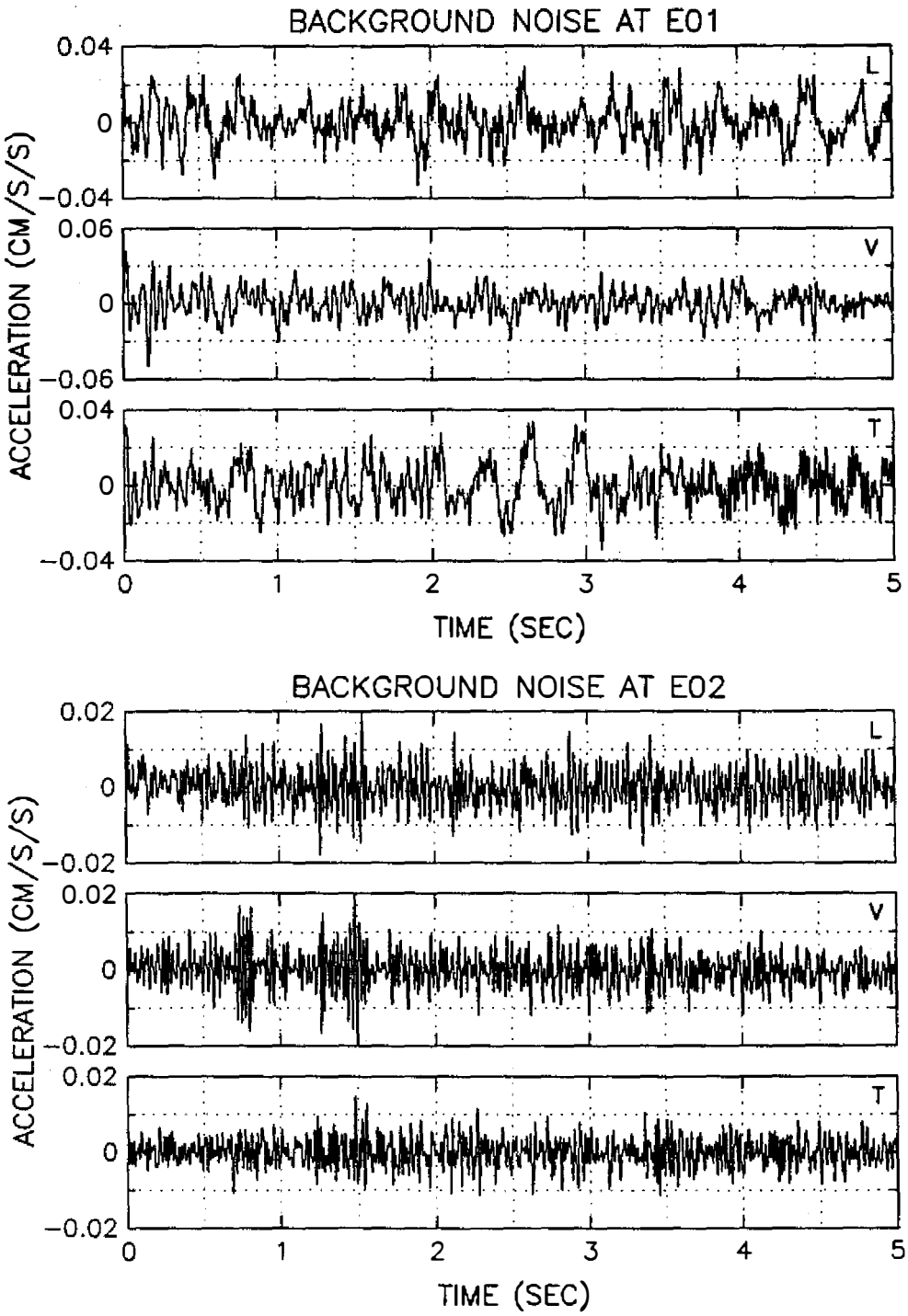

Fig. 4. The time histories of background noise at E01 and E02.

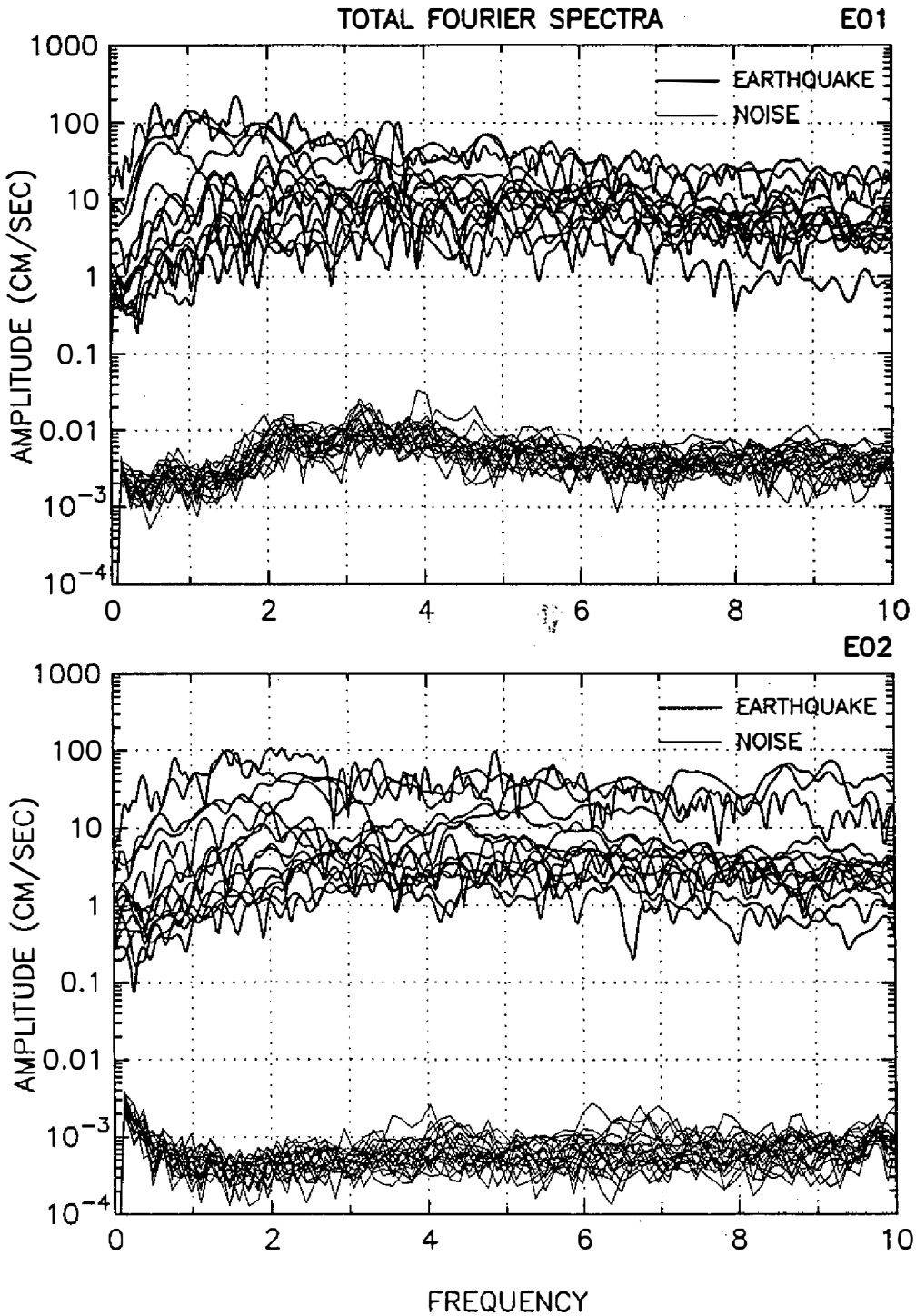

Fig. 5. Comparisons of Fourier amplitude of signal and noise at stations E01 and E02.

4. RESULTS AND DISCUSSION

The Fourier spectra of acceleration at stations E01 and E02 are shown in Figure 6. The spectra of these fifteen events were arranged according to their backazimuths which increased monotonously from the top to the bottom. The thick line in Figure 6 represents the spectrum of E01 and the thin line represents that of E02. Each event is plotted in one box. Those boxes connected together belong to the same group. In the same group, all the events have similar epicenter distance and backazimuth. The Fourier spectrum in each box was normalized by its peak and the peak value is also given at the left side of the corresponding box. In general, the spectrum on a rock site E02 is smaller and smoother than that on a soil site E01. Among these events, except in earthquake 25, none of any other events have similar spectral shape. Earthquake 25 is the farthest one in this study and its epicenter distance is about 97 *km*. Although the spectrum at E02 is smaller than that at E01, the spectra at these two stations have similar shapes. It seems to be a reasonable result, because the great distance and small ground acceleration are not expected to result in non-linear amplification or large variation in ground motion at E01 and E02. The next close events are earthquakes 40, 41 and 45. In events 40 and 45, E01 and E02 have similar spectra at high frequencies but quite different content at low-frequencies. The predominant frequency of both events shifts to the low-frequency end. A similar shift also occurs at earthquake 39. The common feature of these events is large ground motion (0.118, 0.142 and 0.218 *g*). Since the frequency shift and large amplitude are the main factors that cause non-linear amplification, several events selected in this study seem to be related to non-linear amplification. However, further investigation is necessary to verify it.

For low ground acceleration and close-to-station events, such as earthquakes 35, 43, 44, 34, 37 and 54, the frequency shift does not happen but the close epicenter distance still causes spectra at E01 and E02 to be different.

Figure 7 illustrates the spectral ratios of E01 and E02. In taking the ratio, we set all the spectral values below 2 *cm / sec* to be 2 *cm / sec*. Choosing this value was a tradeoff. If we chose a too large value, some of true peaks would have been removed. On the other hand, if too small a value was chosen, it could not effectively remove the pseudo peaks. After several tests, we selected a value of 2 *cm / sec*. This process only removes the very unstable peaks and doesn't provide any guarantee that all significant peaks have been retained or all unwanted pseudo peaks removed.

In Figure 7, all the ratios are normalized to the same scale. The maximum spectral ratio is 12.5 at 3.5 *Hz* in earthquake 29. Since the spectra of E02 at this frequency is small, it might be a pseudo peak. A similar case may have happened in earthquake 54 at 1.5 *Hz*. Excluding these two cases, the amplification factors are less than 9. From group 1 to 10, we cannot find systematic variation of amplification factors. Two possible explanations are: (1) some of these earthquakes are offshore events which cannot be located precisely by the TTSN (Taiwan Telemetered Seismic Network); (2) in many cases, it seems to have non-linear amplification which shifted the frequency contents differently at E01 and E02. The phenomenon of frequency shifting is clear in event 40. In Figure 8, we plot the total spectra

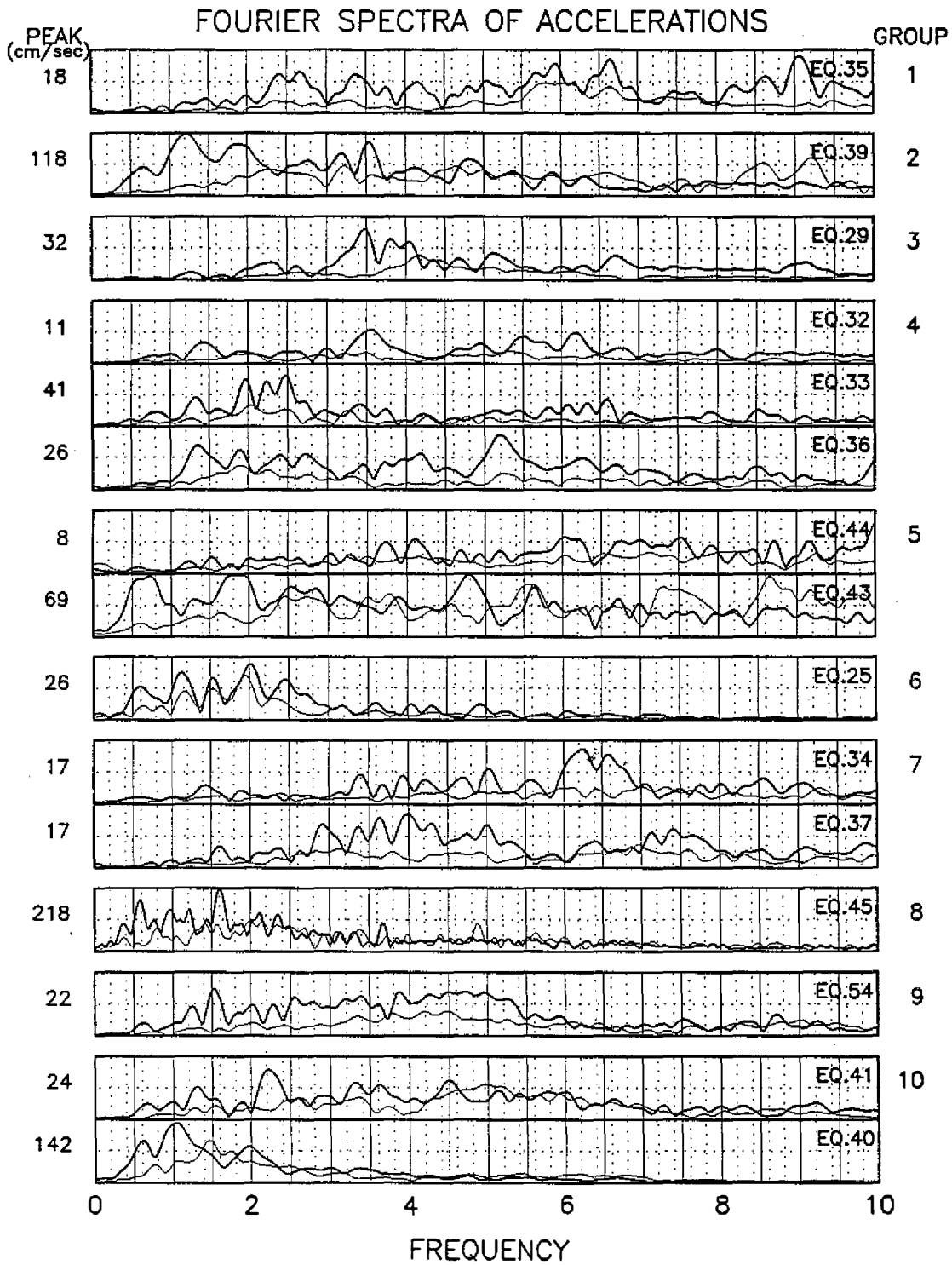

Fig. 6. The Fourier spectra of acceleration at E01 and E02 for fifteen events. The thick line represents spectra at E01. The thin line represents spectra at E02.

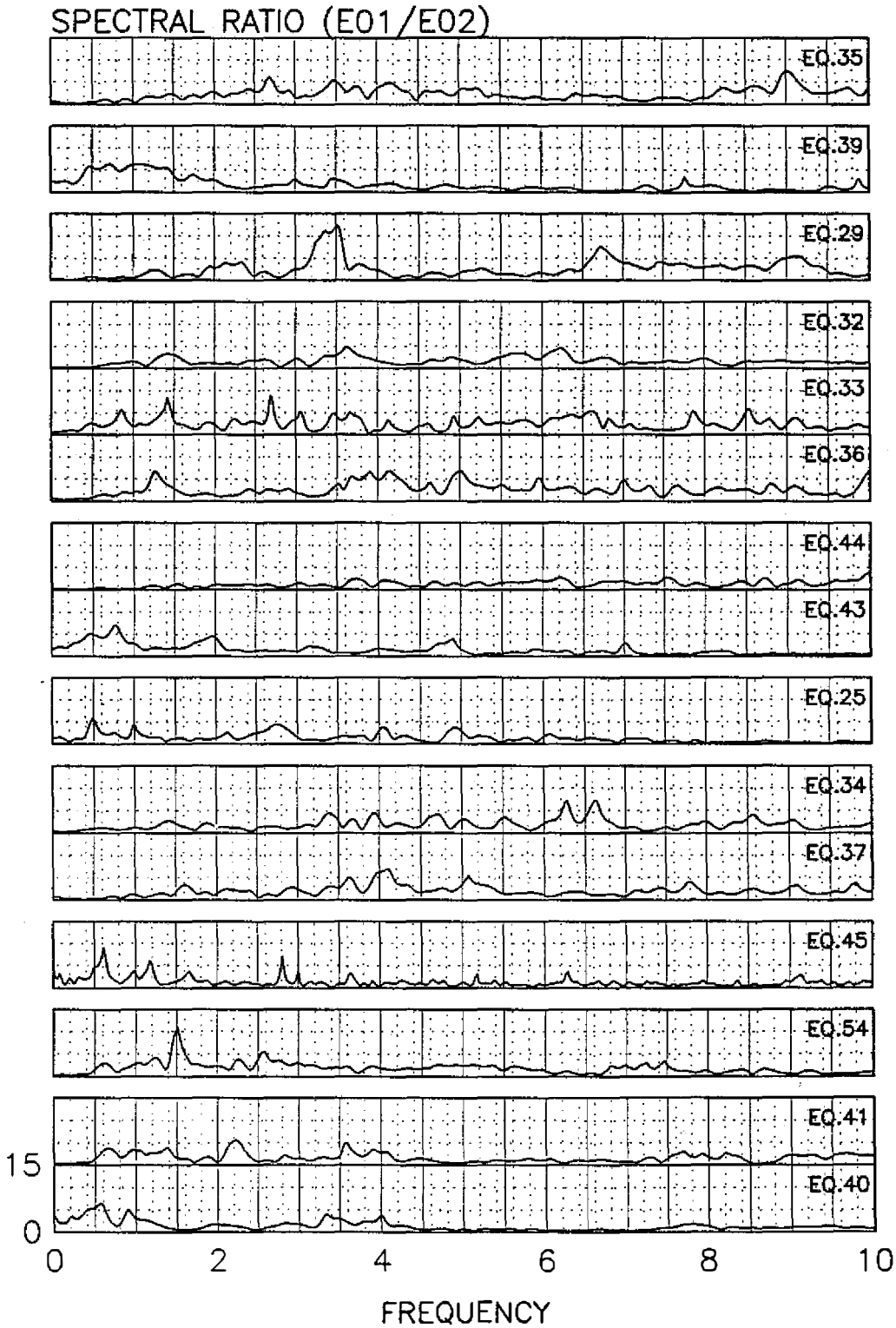

Fig. 7. The E01 / E02 spectral ratios for fifteen events.

of event 40 at seven stations which are configured along a line. In general, the spectra of the soil site have shifted to the low-frequency end vis-á-vis the corresponding spectra of the rock site E02.

In order to compare the spectral ratio in the same group, four groups which have more than one event are re-plotted in Figure 9. In group 4, the similarity is relative low. One possible reason is because of pseudo peaks may exist in the spectral ratio. The other reason is due to the poor hypocenter locations of these offshore events. Poor similarity in group 5 was explained by near-distance effects. Here, the spectral ratio is no longer site-dependent only, because the source and raypath effects become as important as the site effects. Furthermore, earthquake 43 is much larger than earthquake 44, therefore, the source effect might be removed in earthquake 44 but not in earthquake 43. In group 7, the epicentral distance is about 30 *km*, the size of earthquake and ground motion levels are similar. Compared with group 5, the similarity is greater. The double peaks between 6 to 7 *Hz* in earthquake 34 might be the true peaks but it is still very difficult to interpret them from the available data. Subgroup 10 is about 70 *km* away from the station E01. Although the ground motion levels are quite different, the spectral ratios are similar. The difference between events 40 and 41 at low frequencies may be caused by the non-linear effects at E01 in event 40. This effect shifts the spectrum of the soil site to the low-frequency end.

5. CONCLUSION

We present a spectral ratio approach to examine the azimuth-dependent site amplification at E01 of a SMART1 station. Although no systematic variations could be found in this data set as the backazimuth changes, the results of our studies still show that site amplification is azimuth-dependent. It is difficult to classify the azimuth-dependent amplification from our results because of two reasons: (1) For those earthquakes close to the station, the spectral ratio method failed because these ratios are dependent on source and raypath as well as the site effects. (2) Spectral ratio method also failed in the presence of non-linear amplification. The spectral shift to the low-frequency end found in earthquakes 39, 40, 43 and 45 was suspected to be related to the non-linear amplification. However, further verification is required.

Acknowledgements This research was supported by the Academia Sinica and the National Science Council under contract NSC-81-0202-M001-03. The support of these organizations is gratefully acknowledged.

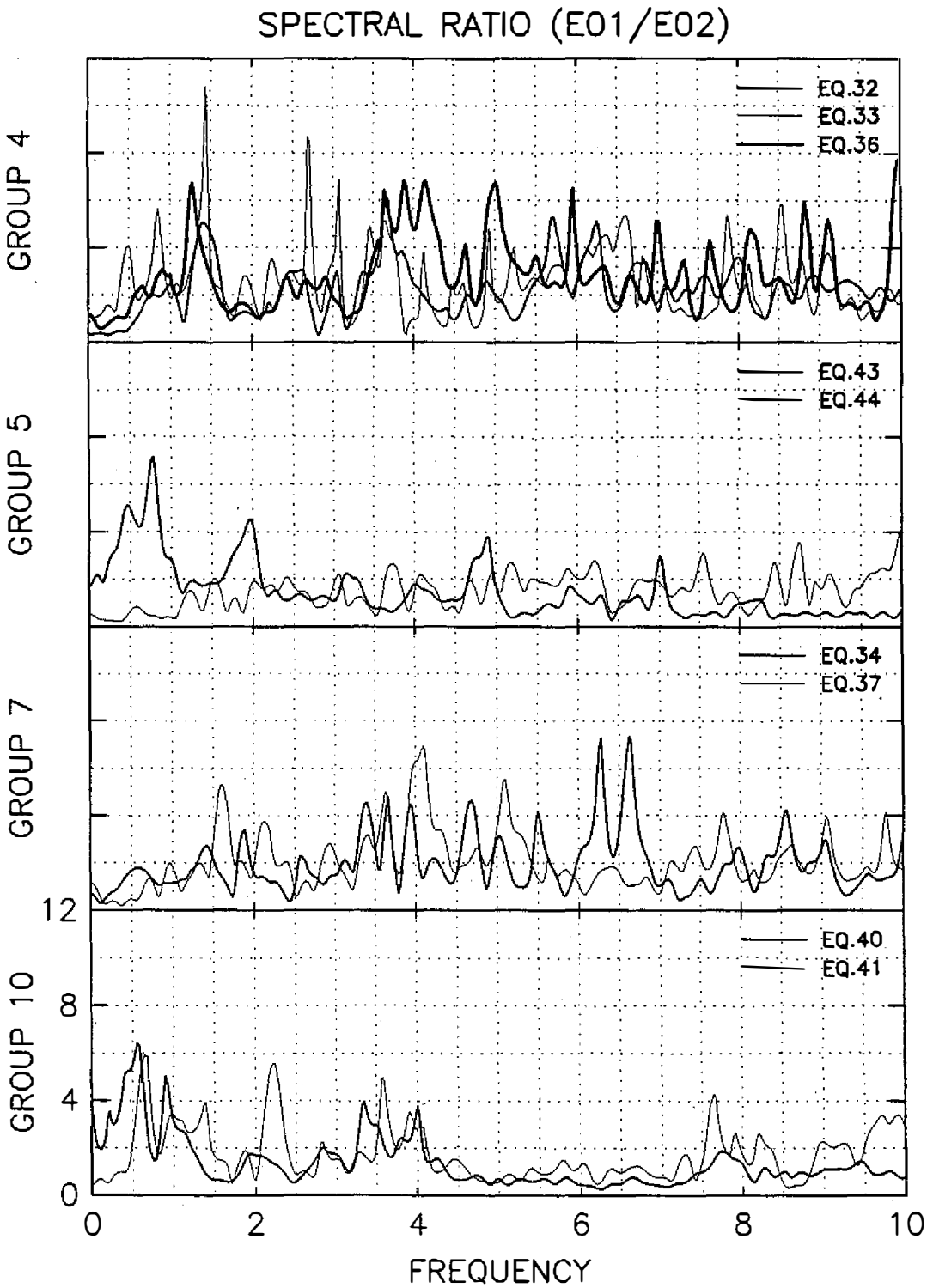

Fig. 8. The Fourier spectra of seven stations of event 40. These stations are configured along a line from station E01 to station E02.

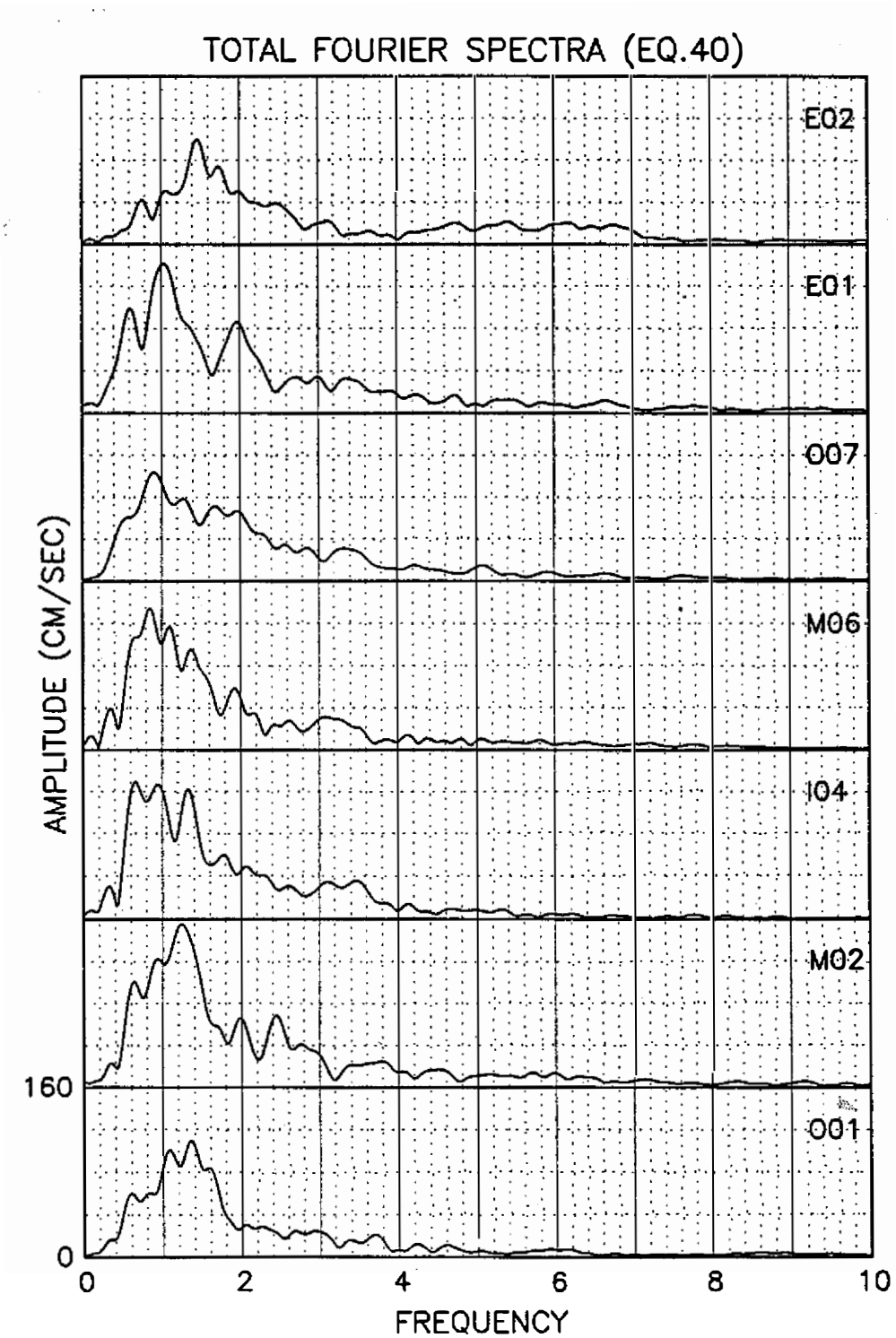

Fig. 9. The E01/E02 spectral ratios of group 4 (event 32, 33 and 36), group 5 (event 43 and 44), group 7 (event 34 and 37) and group 10 (event 40 and 41).

REFERENCES

Aki K., 1988: Local site effects on strong ground motion, in Earthquake Engineering and Soil Dynamics II- Recently Advances in Ground Motion Evaluation, J.L. Vonthun (Editor), geotechnical special Publication No. 20, Am. Soc. Civil Eng., New York, pp. 103-155.

Bonamassa, O. and J.E. Vidale, 1991: Directional site resonances observed from aftershocks of the 18 October 1989 Loma Prieta earthquake, *Bull. Seis. Soc. Am.*, **81**, 1945-1957.

Boore, D. M., 1972: A note on the effect of simple topography on seismic waves, *Bull. Seis. Soc. Am.*, **70**, 305-321.

Burridge, R., F. Mainardi, and G. Servizi, 1980: Soil amplification of plane seismic waves, *Phys. Earth Planet. Int.*, **22**, 122-136.

Campbell, K.W., 1989: The dependence of peak horizontal acceleration on magnitude, distance and site effects for small magnitude earthquake in California and Eastern North America, *Bull. Seis. Soc. Am.*, **79**, 1311-1338.

Chiu, H.C. and H.C. Huang, 1992: Effects of the canyon topography on ground motions at Feitsui Dam site, *Bull. Seism. Soc. Am.* (in press).

Kamiyama, M. and E. Yanagisawa, 1986: A statistical model for estimating response spectra of strong earthquakes ground motion with emphasis on local soil condition, *Soil and Foundations*, **26**, 16-32.

Modiano, T., 1980: Sismotectonique des Pyrenees occidentales. Etude detaillee du contenu spectral des ondes de volume dans la region focale, These de 3eme cycle, Univ. Sci. Med. Grenoble, 188pp (in French).

Seed, H.B., C. Ugas, and J. Lysmer, 1976: Site-dependent spectra for earthquake-resistant design, *Bull. Seis. Soc. Am.*, **66**, 221-243.

Trifunac, M.D., 1973: Scattering of plane SH waves by a semi-cylindrical canyon, *Int. J. Earthquake Eng. Struct. Dyn.*, **1**, 267-281.

Trifunac, M.D. and V.W. Lee, 1990: Frequency dependent attenuation of strong earthquake ground motion. *Int. J. Soil Dynamics and Earthquake Eng.*, **1**, 3-15.

Wen, K.L. and Y.T. Yeh, 1984: Seismic velocity structure beneath the SMART1 array, *Bull. Inst. Earth Sci.*, Academia Sinica, **4**, 51-72.

Wong, H.L., 1982: Effect of surface topography on the diffraction of P. SV and Rayleigh waves, *Bull. Seis. Soc. Am.*, **72**, 1167-1183.

Wong, H.L., and P.C. Jennings, 1975: Effect of canyon topography on strong ground motion, *Bull. Seis. Soc. Am.*, **65**, 1239-1257.

隨方位變化的場址放大效應

邱宏智
中央研究院地球科學研究所
黃蕙珠
中央大學地球物理研究所

摘　要

本研究使用 SMART-1 強震儀陣列中的兩個測站所收錄的地震記錄探討場址放大效應隨震央方位的變化情形。本文共選用了十五個地震，乃因它們同時啓動 E01 土層測站和 E02 岩盤測站的強震儀。首先，我們將 E01 和 E02 的記錄分別截取一段包含直接 S 波的波線，並求其傅氏振幅譜，然後再求 E01 對 E02 之頻譜比。由於岩盤測站受場址效應的影響較小，因此頻譜比可將大部份的震源及波傳路徑效應消除，而呈現 E01 的場址放大效應。

爲了比較不同震央距及方位角對放大效應的影響，我們將這些地震分成十組，使同一組之地震具有相近的震央距及反方位角，分析這些地震之結果顯示：不同組資料有不同之放大效應，而各組間並無明顯的系統性差異。至於同一組的地震，預期應有相似的頻譜比，但所得的結果卻只有部份組之部份頻段存在相似性，而這些異常現象可歸因於近震源及非線性放大兩種效應所致。